

# DeepMDV: Learning Global Matching for Multi-depot Vehicle Routing Problems

Saeed Nasehi, Farhana Choudhury, Egemen Tanin

*The University of Melbourne*

{snasehibasha@student., farhana.choudhury@, etanin@} unimelb.edu.au

**Abstract**—Due to the substantial rise in online retail and e-commerce in recent years, the demand for efficient and fast solutions to Vehicle Routing Problems (VRP) has become critical. To manage the increasing demand, companies have adopted the strategy of adding more depots. However, the presence of multiple depots introduces additional complexities, making existing VRP solutions suboptimal for addressing the Multi-depot Vehicle Routing Problem (MDVRP). Traditional methods for solving the MDVRP often require significant computation time, making them unsuitable for large-scale instances. Additionally, existing learning-based solutions for the MDVRP struggle with generalizability and fail to deliver high-quality results for scenarios involving a large number of customers. In this paper, we propose a novel solution for MDVRP. Our approach employs an attention mechanism, featuring a decoder with two key layers: one layer to consider the states of all vehicles and learn to select the most suitable vehicle based on the proximity of unassigned customers, and another layer to focus on assigning a customer to the selected vehicle. This approach delivers high-quality solutions for large-scale MDVRP instances and demonstrates remarkable generalizability across varying numbers of customers and depots. Its adaptability and performance make it a practical and deployable solution for real-world logistics challenges. Code is available at: <https://github.com/SaeedNB/DeepMDV.git>

**Index Terms**—Vehicle Routing Problem, Spatial data management, Combinatorial optimization.

## I. INTRODUCTION

The rapid growth of online retail and e-commerce has significantly increased delivery requests in urban areas, with thousands being processed every minute [1]. In 2022, Manhattan experienced over 2.4 million daily delivery requests [2], equating to more than 3,000 deliveries every minute during a 12-hour workday. This highlights the need for solutions that are not only effective but also capable of producing results in a few seconds. Even algorithms that take minutes to compute fall short in handling such massive, real-time scheduling demands, as delays can quickly cascade, causing significant disruptions across the entire logistics network. Moreover, in large cities like New York City, for example, over 30,000 delivery trucks are active, each covering more than 12,000 miles annually [3], which emphasizes the critical need for optimizing delivery routes, as even a 1% reduction in driving distances could save over 3.6 million miles of travel each year.

The delivery problem is commonly modeled as the Vehicle Routing Problem (VRP), where vehicles are tasked with delivering parcels to requesters [4]. These routing queries typically originate from warehouses (depots) in e-commerce, while destinations are workplaces or homes. The main challenge in

VRP lies in determining the optimal sequence of customer visits, where the vehicles have capacity constraints, ensuring efficient routes to fulfill requests.

In response to growing demands, companies are increasingly expanding their networks by establishing additional depots [5]. The Multi-Depot Vehicle Routing Problem (MDVRP) extends the complexity of the single-depot VRP, both of which are NP-hard. While the VRP focuses solely on determining the optimal path for customer visits, the MDVRP adds complexity by requiring the identification of both the starting depot and the routes for a fleet of vehicles to satisfy all customer demands (e.g., deliveries). This process typically adheres to specific objectives, such as minimizing the total distance traveled [6]. The inclusion of multiple depots significantly increases the problem's difficulty, as it expands the decision space and complicates the search for optimal solutions.

MDVRP solutions are broadly categorized into two approaches based on their methodology: **i) MDVRP as Multiple Single-depot VRP:** Known as the Clustering-then-Routing, this spatial partitioning approach divides the problem into clusters, each associated with an individual depot [7]. Each cluster is then solved as a VRP using existing techniques. **ii) MDVRP as a Unified Instance:** In this method, (meta-)heuristic or learning-based solutions are designed to handle the MDVRP in its entirety, providing routes for each customer and identifying the depot that serves each customer [8], [9].

The clustering-then-routing approach is a straightforward approach for extending VRP solutions to multi-depot scenarios. It uses a distance-based clustering algorithm to divide the problem into multiple single-depot VRPs, which are then solved using existing VRP solutions. While this method enables easy application of any VRP solution to the MDVRP by dividing the problem into clusters, it often results in suboptimal outcomes. This is due to its lack of a global perspective, which can lead to imbalanced workloads, suboptimal customer assignments near cluster boundaries, and underutilized vehicles. Consequently, total travel distances increase, and overall efficiency declines. While deep learning (DL) solutions show high performance for single-depot VRP by quickly mapping problem instances to (near-)optimal solutions and can be applied to large instances [10]–[12], there is no such existing approach for MDVRP. As the existing DL solutions for VRP can only be applied to MDVRP by clustering-then-routing approach, they suffer from all the drawbacks mentioned above.

Solutions in the second category can be further divided

into two main groups: (meta-)heuristic approaches [13]–[15] and machine learning-based solutions [8]. The (meta-)heuristic approaches rely on well-established methods, such as local search [16]–[18], genetic algorithms [7], [14], ant colony optimization [19], [20], large neighborhood search [21], and tabu search [22], [23]. These methods follow a construction-destruction-improvement cycle [24], iteratively refining solutions until a predefined time limit is reached [13]. Given the vast search space, they often require numerous iterations and substantial memory resources to achieve satisfactory results.

To the best of our knowledge, Arishi et al. [8] is the only learning-based solution for MDVRP, modeling the problem as a Multi-agent Deep Reinforcement Learning task. Although their method delivers high-quality solutions for instances with fewer than 100 customers, it is not effective for larger ones. Moreover, the resource-intensive nature of multi-agent systems makes it difficult to train this model for large instances.

We are the first to propose an efficient and effective deep learning-based solution for the MDVRP that, unlike previous methods [8], can efficiently address large-scale MDVRP instances. The novelty of our approach is that, it allows for the simultaneous generation of multiple tours, each originating from a different depot. This approach evaluates customer assignments to tours by considering not only the state of the tour from the nearest depot but also the tours from other depots. It follows a two-step decision process: first, it selects the most appropriate tour by evaluating the states of the nearest customers, and then assigns a customer to that tour. As a result, customers can be assigned to the most suitable tour, even if it originates from a more distant depot, enhancing efficiency and solution quality. The two-step decision process not only makes our method effective for solving the MDVRP, but also enables it to efficiently handle the single-depot VRP.

In this paper, we present **DeepMDV**, a deep learning-based framework designed to solve the Multi-depot Vehicle Routing Problem. This model employs a transformer architecture featuring a decoder with two specialized layers: the Vehicle Selection and Local Context Generation Layer (VSLCGL) and the Node Selection Layer (NSL). The VSLCGL layer is tasked with selecting the appropriate tour from a list of available tours to pick the next customer, while the NSL identifies the most suitable customer for the selected tour. After assigning all customers to their respective tours, the optimal sequence for visiting customers within each tour is determined. This ordering can be approached through various methods, ranging from heuristic techniques to learning-based solutions.

The VSLCGL is a critical component of this model, enabling the simultaneous generation of multiple tours, each originating from a different depot. It begins by identifying the  $k$  nearest unvisited neighbors to the last customer added to each tour. Then, it computes a compatibility score between each selected customer and the tours, evaluating how well a customer matches a tour based on proximity, demand, and route efficiency. The vehicle with the highest compatibility score is chosen for the next assignment.

Additionally, the VSLCGL generates a local context em-

bedding for each neighboring customer, which, when combined with the customer’s initial embedding produced by the encoder, enables the Node Selection Layer (NSL) to fine-tune the compatibility of nearby customers. This adjustment prioritizes those customers who are best suited to the selected tour, while reducing the compatibility for those that are better aligned with other tours. This approach ensures that the status of all neighboring customers is evaluated in the context of all available tours, rather than selecting the next node solely based on the state of the selected tour and its associated customers.

Our method employs a two-stage training approach: initially, customers are partitioned into multiple tours, and then the optimal sequence for visiting customers within each tour is determined. Our method utilizes the Attention Model (AM) [25] to compute the minimum travel distance for a set of customers and a depot within each tour. Our experiments show that as the size of MDVRP instances increases, the spatial distribution of customers and the depot within a tour deviates from uniformity. This deviation causes the AM, originally trained on a uniform distribution, to struggle with maintaining high solution quality. To address this issue, we developed a new procedure for training AM, leading to a significant improvement in solution quality for larger MDVRP instances.

The contribution of this paper can be outlined as follows:

- 1) To the best of our knowledge, DeepMDV is the first learning-based approach for the large-scale MDVRP that effectively integrates vehicle and node selection. By leveraging contextual information, our method efficiently identifies the next customer for each vehicle, aiming to minimize the total driving distance for vehicles departing from any depot.
- 2) We propose a new training approach for the AM to enhance its capability to deliver high-quality solutions for each tour generated by our model.
- 3) DeepMDV shows strong generalizability, delivering high-quality solutions for MDVRP instances with many hundreds of customers in a short timeframe. We validate our method on both synthetic (uniform and skewed distributions) and real-world MDVRP instances, showing that it can solve problems with 1,000 customers and up to four depots in less than 5 seconds, producing solutions that are shorter than state-of-the-art approaches.
- 4) The generalizability of our method extends beyond the number of customers. It efficiently solves MDVRP instances with varying numbers of depots than those used during training, making it also highly effective for single-depot VRP, as well.

## II. RELATED WORK

This literature review focuses on (meta-)heuristic and learning-based approaches specifically designed for the MDVRP. Additionally, we discuss state-of-the-art learning-based methods for single-depot VRP in Section II-C and present their limitations when applied to MDVRP. While exact algorithms, such as branch-and-bound [26], integer linear programming [27], and solvers like Gurobi can theoretically

solve MDVRP, their high computational demands make them impractical for instances exceeding 50 customers.

#### A. Heuristic and meta-heuristic methods

Authors in [19] developed a parallel algorithm based on Ant Colony Optimization (ACO) to enhance computational efficiency and solution quality for MDVRP. Ombuki-Berman et al. applied Genetic Algorithms (GA) to address MDVRP [9], while authors in [7] further refined GA-based approaches by grouping customers based on their proximity to the nearest depot before optimizing the routes within each cluster using GA. Vidal [14] introduced a hybrid method combining local search with GA, leveraging the strengths of both techniques to produce high-quality solutions for VRP, which can also be applied to MDVRP. Lahyani et al. [28] introduced a hybrid adaptive large neighborhood search algorithm that combined some novel improvement procedures to enhance solution quality. Tabu Search (TS) has also been used to solve MDVRP. Cordeau et al. [29] proposed a TS algorithm with the randomly generated initial solution for the MDVRP. Escobar et al. [30] proposed an enhanced strategy and used a hybrid Granular TS that leverages various neighborhood and diversification strategies to improve the quality of the initial solutions.

These methods typically follow a construction-destruction-improvement pattern, where an initial feasible solution is iteratively refined until an acceptable solution is obtained. Despite their effectiveness and interpretability, these methods often require substantial memory and long computation times to generate high-quality solution [11], making them less practical for real-life and large-scale scenarios.

#### B. Learning-based methods

Deep learning-based solutions use the representation learning capabilities of neural networks to rapidly map problem instances to (near-)optimal solutions. These approaches often employ techniques like graph neural networks [31], [32], attention mechanisms [33], and reinforcement learning to model the combinatorial nature of the problem and learn complex decision-making strategies. Although many solutions have been developed for VRP and its variants, such as Pickup and Delivery [1], [34], [35], there is a significant gap in learning-based methods specifically addressing the MDVRP.

To the best of our knowledge, Arishi et al. [8] have proposed the state-of-the-art learning-based solution for the MDVRP. They developed a Multi-agent Deep Reinforcement Learning (MADRL) model using an attention-based transformer model, trained with a policy gradient method. This approach falls short in providing high-quality solutions for MDVRP instances with several hundred customers and is hindered by significant computational resource requirements during both the training and inference phases for large instances. The high computational complexity and substantial memory demands make it challenging to train this model for MDVRP instances with more than 100 customers and four depots, as an example.

#### C. Extending VRP to solve MDVRP

Notably, the partitioning-then-routing strategy has recently emerged as a popular approach in learning-based methods for solving large-scale VRPs [10], [11], [36]–[39]. Hou et al. [11] introduce the Two-stage Divide Method (TAM) designed for large-scale VRP scenarios which autoregressively partitions the VRP instance into sub-TSPs. In contrast, Ye et al. [10] propose Global and Local Optimization Policies (GLOP) to combine non-autoregressive global partition with autoregressive local construction policies to first learn the partitioning and then learn to solve sub-TSPs. None of these methods are capable of effectively addressing MDVRP instances directly.

Although distance-based clustering [7], followed by applying one of the many proposed VRP solutions [10], [11], [25], [40], [41], is a straightforward strategy for solving MDVRPs, it often leads to suboptimal results. This approach neglects global optimality, leading to imbalanced workload distribution among depots and inefficient customer assignments near cluster boundaries. Consequently, some vehicles may be underutilized, leading to increased total travel distance and reduced solution's overall efficiency. This highlights the necessity of designing a model specifically for MDVRP. In our experiments, we use these methods as baselines to benchmark and evaluate the performance of DeepMDV.

### III. PROBLEM DEFINITION

The Vehicle Routing Problem (VRP) is a combinatorial optimization challenge that involves efficiently routing a fleet of vehicles from a designated depot to meet all customer demands while adhering to specific objectives and various constraints. In the Capacitated Vehicle Routing Problem (CVRP), vehicles with limited carrying capacities must fulfill customer demands.

The Multi-depot Vehicle Routing Problem (MDVRP) generalizes the traditional CVRP by incorporating multiple depots from which vehicles can start their routes. Depending on the problem's constraints, vehicles may either return to their starting depot (closed tour) or finish at any depot (open tour).

In this paper, we propose a solution for the MDVRP with closed tours. This problem involves a set of depots  $\mathcal{D}$  and a set of customers  $U$ . The objective is to determine a set of routes for a fleet of vehicles, where each vehicle starts and ends its route at a depot, aiming to minimize the total traveling distance while satisfying all customer demands and vehicle constraints.

Let  $V$  be a set of vehicles, where each vehicle  $v \in V$  has a capacity  $C_v$ , and each customer  $i \in U$  has a demand  $\delta_i$ . The distance between any two nodes  $i$  and  $j$ , where  $i, j \in \mathcal{D} \cup U$ , is denoted by  $e_{ij}$ . We define  $x_{ijv} \in \{0, 1\}$  as a binary decision variable that equals 1 if vehicle  $v$  travels from  $i$  to  $j$ , and 0 otherwise. Let  $z_j$  represent an auxiliary variable indicating the cumulative load of the vehicle after serving customer  $j$ , the MDVRP problem can then be formulated as follows:

$$\text{Minimize } \sum_{i \in \mathcal{D} \cup U} \sum_{j \in \mathcal{D} \cup U} \sum_{v \in V} e_{ij} x_{ijv} \quad (1)$$

$$\sum_{v \in V} \sum_{i \in \mathcal{D} \cup U} x_{ijv} = 1, \forall j \in U \quad (2)$$

$$\sum_{i \in \mathcal{D} \cup U} x_{ijv} = \sum_{j \in \mathcal{D} \cup U} x_{jiv}, \forall j \in U, \forall v \in V \quad (3)$$

$$\sum_{i \in U} x_{div} = 1, \sum_{i \in U} x_{idv} = 1, \forall d \in \mathcal{D}, \forall v \in V \quad (4)$$

$$\sum_{j \in U} \delta_j \sum_{i \in \mathcal{D} \cup U} x_{ijv} \leq C_v, v \in V \quad (5)$$

$$z_j \geq z_i + n_i - M(i - x_{ijv}), \forall i \neq j, \forall v \in V \quad (6)$$

Equation 1 defines the objective of minimizing the total cost of all routes. Equation 2 ensures that each customer is visited exactly once by one of vehicles, while Equation 3 enforces that if a vehicle arrives at a customer, it must also depart from that customer. Equation 4 specifies that each vehicle's route must start and end at a specific depot. Equation 5 ensures that the total demand serviced by each vehicle does not exceed its capacity. Finally, Equation 6 prevents the formation of subtours, thereby guaranteeing a valid route.

#### IV. METHODOLOGY

##### A. Definition of tours

Before introducing the proposed algorithm, it is essential to define the concepts of standby, initiated, active, and inactive tours. A **standby tour** is a tour that has not yet been assigned any customers, representing a vehicle at the depot with full capacity. An **initiated tour** is a tour that has at least one assigned customer and can accept more. Assigning a customer to a standby tour turns it into an initiated tour. The term **Active tours** refers to tours that are either in standby or have already been initiated. While the active tour list can theoretically contain any number of tours, having multiple active tours originating from the same depot simultaneously reduces training efficiency without improving solution quality. To streamline the process, we assume only one active tour can exist per depot at any given time. Consequently, the number of active tours at any step is limited to the total number of depots ( $|\mathcal{D}|$ ), with no two active tours originating from the same depot. **Inactive tours** is a list of tours that no longer accept new customers, having selected the depot node as their final stop. When an active tour becomes inactive, a new standby tour from the same depot replaces it in the list of active tours.

##### B. Markov decision process model

We model the MDVRP problem as a Markov Decision Process (MDP), defined by the 4-tuple  $M = \{S, A, T, R\}$ . The detailed definition of the state space  $S$ , the action space  $A$ , the transition function  $T$ , and the reward function  $R$  are provided below.

**State:** State  $s_t \in S$  consists of two components,  $(H, \Phi_t^a)$ . The first component,  $H$ , describes the embedding of nodes, expressed as  $H = \{h_0, \dots, h_n\}$ . Each embedding comprises a vector that captures the location of the node, and a scalar value that defines the demand of the customer. The demands for all depot nodes are considered as zero. The second component,  $\Phi_t^a$ , represents the state of all active tours at step  $t$ , denoted

as  $\Phi_t^a = \{\phi_1^t, \dots, \phi_m^t\}$  where  $m \leq |\mathcal{D}|$ . The state of each active tour at step  $t$  is described by  $\phi_i^t = \{h_{d_i}, h_{v_i^{(t-1)}}, c_i^t\}$  which includes the embedding of depot it started from ( $d_i$ ), the embedding of the last node added to the tour ( $v_i^{(t-1)}$ ), and remaining available capacity ( $c_i^t$ ).

**Initial state:** The initial state is defined as  $(H, \Phi_0)$ , where  $H$  represents the node embeddings, and  $\Phi_0$  denotes the initial state of all active tours at step  $t = 0$ . The state of each active tour at this step is described by  $\phi_i^0 = \{h_{d_i}, h_{d_i}, C\}$ , where  $h_{d_i}$  is the embedding of the depot node for the tour, and  $C$  indicates the maximum available capacity.

**Action:** The action at step  $t$  involves selecting a tour from the current list of active tours and assigning a new node to it. In other words, the action  $a^t \in A$  is represented as  $(\phi_i^t, n_j)$ , indicating that node  $n_j$  is added to tour  $\phi_i^t$ .

**Transition:** The transition rule is to update the state  $s_t$  to  $s_{t+1}$  based on performed action  $a_t = (\phi_i^t, n_j)$ . In this process, the last added node of the selected tour is changed to  $n_j$ , and the remaining capacity of the tour is updated as  $c_i^{t+1} = c_i^t - d_{n_j}$ . If the selected node is the depot, the current tour  $\phi_i$  is marked as inactive and moved to the list of inactive tours. If the total number of tours has not yet reached the optimal maximum (as detailed in Section V-A), a new standby tour originated from the same depot replaces it in the active tour list.

**Reward:** The reward function for each problem instance is computed after all customers are assigned to tours and is defined as the negative sum of the minimum Euclidean distances for all tours. Since each tour begins and ends at a depot, the reward for each tour corresponds to the total travel distance of the Hamiltonian cycle with the minimum length within that tour. Mathematically, this is expressed as:

$$R = - \sum_{\phi_i \in \Phi} \text{MinCycleLength}(\phi_i) \quad (7)$$

where  $\Phi$  is the list of tours, and  $\text{MinCycleLength}(\phi_i)$  represents the travel length of the Hamiltonian cycle with the shortest distance for tour  $\phi_i$ . Finding the Hamiltonian cycle with the shortest length, also known as solving the Traveling Salesman Problem (TSP), is an NP-hard problem. However, by dividing the entire problem space into multiple tours, our method enables the use of heuristic or machine learning-based solutions specifically designed for TSP, resulting in efficient and effective method for calculating rewards.

#### V. DEEPM DV

Figure 1 shows the framework of the proposed solution. Our approach focuses on learning a stochastic policy  $p_\theta(a_t|s_t)$ , represented by a deep neural network with trainable parameter  $\theta$ . This policy partitions customers into multiple tours, ensuring each customer is assigned to one of the tours by the end of the process. Each tour is associated with a specific depot, and the partitioning process generates  $m$  distinct groups of customers. The optimal visiting sequence within each tour is then determined to minimize travel distance.

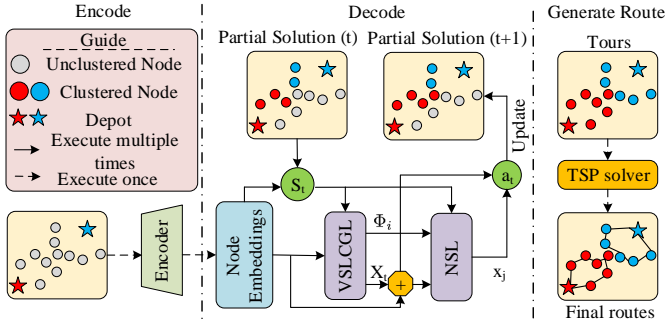


Fig. 1. The DeepMDV framework leverages the embeddings produced by encoder and the partial solution to generate local context and identify the candidate tour for the next node through VSLCGL. The node embedding, combined with the local context, used to choose the next best customer for the candidate tour. Once all customers are assigned, each tour is optimized using a TSP solver to minimize travel length. Best viewed in color.

Our policy network  $p_\theta$  is composed of an encoder and a decoder. The decoder includes a Vehicle Selection and Local Context Generation Layer (VSLCGL) along with a Node Selection Layer (NSL). Given that the problem instance remains fixed during the decision-making process, the encoder runs only once at the beginning, and its outputs are used in subsequent steps ( $t > 0$ ) for tour construction.

At each step, the policy network selects a tour ( $\phi_i^t$ ) via VSLCGL and a customer ( $n_j$ ) for that tour through NSL, forming the action to update the partial solution and states. This process repeats until all customers are served. The visiting order within each tour is then optimized using either a trained AM [25] on TSP or solvers like LKH3 [15]. Partitioning the problem into tours and optimizing sequences within them enhances generalizability of the model [11].

#### A. Optimal maximum number of tours.

In the MDVRP, each tour must adhere to vehicle capacity constraints to prevent exceeding the vehicle's capacity. A new constraint can be defined to determine the optimal maximum number of tours before processing. Inspired by the approach proposed for the VRP [11], we introduce this constraint for the MDVRP. For an MDVRP instance with  $|U|$  customers and  $|\mathcal{D}|$  depots, where  $C$  represents the maximum vehicle capacity and  $\delta_i$  denotes the demand of customer  $i$ , the optimal upper limit for the number of tours can be determined as follows:

$$l_{max} = \lceil \frac{\sum_{i=0}^{|U|} \delta_i}{C} \rceil + |\mathcal{D}| \quad (8)$$

The first part of the equation determines the minimum number of tours needed to meet all demands. Since the optimal MDVRP solution may have up to  $|\mathcal{D}|$  partially loaded tours, we add the number of depots to the minimum number of tours needed. This allows vehicles originating from each depot have the flexibility to deactivate an active tour before reaching their capacity limit, entails in a more efficient solution. Our experiments show that predefining the optimal maximum number of tours can speed up model convergence. Note that,  $l_{max}$  represents the maximum number of tours allowed. Depending on the problem instance and the model, the actual number of tours can vary but will not exceed this limit.

**Masking function for initiating a standby tour:** The first step to satisfy the optimal maximum number of tour constraint, is defining a masking function for allowing whether a standby tour in active tours is allowed to take customers. A standby tour can turn into an initiated tour if the summation of the number of initiated tours and inactive tours is less than  $l_{max}$ .

**Masking function for deactivating an active tour:** The second step to satisfy the optimal maximum number of tour constraint, is defining a masking function for deactivating an initiated tour. This function determines whether a tour  $\phi_i$  with a total remaining capacity of  $0 < c_i \leq C$  can be deactivated by selecting the depot node as the next stop. To create a flexible masking function, we define a threshold at decoding iteration  $t$  named  $\mathcal{T}_t$ . This threshold will be used in Equation 25 to determine whether a tour should be deactivated or remain active. Let  $\phi_i$  denote an inactive tour with its unused capacity defined as wasted capacity  $w_{\phi_i}$ . Then, given the set of all inactive tours to iteration  $t-1$  ( $\mathcal{L}_i^{(t-1)}$ ), the total capacity that can be wasted at step  $t$  is calculated as follow:

$$\eta_t = l_{max} * C - \sum_{i=0}^n \delta_i - \sum_{\phi \in \mathcal{L}_i^{(t-1)}} w_{\phi} \quad (9)$$

So, the threshold  $\mathcal{T}$  at iteration  $t$  can be defined as:

$$\mathcal{T}_t = \frac{\eta_t}{l_{max} - |\mathcal{L}_i^{(t-1)}|} \quad (10)$$

#### B. Encoder

The encoder follows the architecture presented by Kool et al. [25] and transforms customers and depots (call it nodes when we refer to both customers and depots) input  $I_i$  into a hidden embedding  $h_i$ . The input of each customer  $i$  comprises its coordinates  $(x_i, y_i)$  and its associated demand  $\delta_i$  while the value of demand for depots is zero. However, unlike Kool et al [25], we transform the node coordinates into polar coordinates with respect to the first depot  $(x_0, y_0)$ . Polar coordinates enhance the model's generalizability by making the representation invariant to spatial transformations such as shifts, rotations, and scaling, enabling the model to capture the relative positioning and angular relationships between nodes rather than relying on their absolute locations. Consequently, the node attributes are represented by the relative Euclidean distance and polar angle, as well as their demand.

$$I_i = \{r_i, \theta_i, \delta_i\} \quad (11)$$

where,

$$r_i = \sqrt{(x_i - x_0)^2 + (y_i - y_0)^2} \quad (12)$$

and,

$$\theta_i = \arctan2(y_i - y_0, x_i - x_0) \quad (13)$$

#### C. Decoder

Our proposed decoder model consists of two key layers: the Vehicle Selection and Local Context Generation Layer (VSLCGL) and the Node Selection Layer (NSL). At each iteration, the decoder is tasked with selecting a pair consisting of

an active tour and a customer. The VSLCGL is responsible for identifying the tour with the highest ‘compatibility’ (explained later) with the unvisited neighbor customers and generating local context. This context assists the Node Selection Layer in choosing the next node for the selected tour, taking into account the status of other ongoing tours.

**Vehicle Selection and Local Context Generation Layer (VSLCGL):** Figure 2 illustrates the architecture of the proposed decoder, highlighting the Vehicle Selection and Local Context Generation Layer (VSLCGL). At each iteration, we identify the  $k$  nearest nodes, denoted as  $\zeta$ , relative to the last customer added to each active tour. This approach aligns with findings that optimal actions in VRP are often concentrated among local neighbors [12]. Then, the embeddings corresponding to these nodes in  $\zeta$ , are extracted from the encoder’s output and serve as queries within the multi-query, multi-head attention mechanism, as follows:

$$q_i = W^{Q_1} h_i, \forall i \in \zeta \quad (14)$$

The keys and values are derived from the state of each active tour as follows:

$$h_\phi = [h_{0\phi}, h_{l\phi}, c_\phi] \quad (15)$$

and,

$$k_j = W^{K_1} h_{\phi_j}, v_j = W^{V_1} h_{\phi_j} \quad (16)$$

Here  $[\cdot, \cdot, \cdot]$  is the horizontal concatenation operator where  $h_{0\phi}$  represents the embedding of the depot of the tour  $\phi$ ,  $h_l$  denotes the embedding of the last added node to the tour, and  $c_\phi$  indicates the remaining capacity of the vehicle undertaking the tour. The queries, keys, and values are defined as follows:

The local context is then calculated as:

$$\mathcal{X}_i = softmax(\frac{q_i k_j^T}{\sqrt{dim_{k_j}}}) v_j \quad (17)$$

The local context plays a vital role in guiding the NSL to prioritize nodes with a higher probability for a selected tour. It provides detailed information about the compatibility of each node with all active tours, ensuring that the model avoids assigning nodes to a tour where they would be better suited for another one. This strategic approach helps the model make more efficient decisions by optimizing the assignment of nodes to tours, thereby improving overall routing efficiency and achieving a globally optimal solution.

In the final step, a multi-query single-head attention mechanism generates the unnormalized log-probabilities (logits) for each pair of tours and neighbor nodes. The query and key for generating logits is defined as:

$$q'_i = W^{Q_2} \mathcal{X}_i, v'_j = W^{K_2} h_{\phi_j} \quad (18)$$

After applying a max pooling layer, the logits for each tour are computed and clipped to the range  $[-A, A]$  (with  $A = 10$ )

using  $\tanh$  function. The tour with the highest probability is selected as the candidate tour to pick the next node.

$$o = \begin{cases} A \cdot \tanh(\text{Max}(\frac{q'_i v'_j{}^T}{\sqrt{dim_{v'_j}}})) & \text{if tour is active} \\ -\infty & \text{Otherwise} \end{cases} \quad (19)$$

and,

$$\phi = \text{argmax}(o) \quad (20)$$

**Node Selection Layer (NSL):** Given  $\phi$  as the selected tour and  $\mathcal{X}$  as the generated local context from the VSLCGL, we apply attention mechanism to select the next node within the specified tour. The input embedding  $h_i$  for this process consists of the tour depot’s embedding and the updated node embeddings, which incorporate the local context. For non-depot nodes, each embedding is enriched by combining their local context with their individual embeddings, effectively encoding the status of all active tours within each node’s representation. This strategy enables the model to account for the current status of all active tours when selecting the next node for a given tour, ensuring that the decision process is informed by the broader tour dynamics. So, the embedding  $h_i$  is defined as follows:

$$h_i = \begin{cases} h_{0\phi}, & i = 0 \\ h_i + \mathcal{X}_i, & i \in \zeta_k \\ h_i, & \text{Otherwise} \end{cases} \quad (21)$$

The query of the attention mechanism in NSL is defined as:

$$q = W^{Q_3} [h_g, h_{0\phi}, h_{l\phi}, c_\phi] \quad (22)$$

Here  $[\cdot, \cdot, \cdot, \cdot]$  is the horizontal concatenation operator where  $h_g$  is the average value of the hidden embeddings of all nodes that are not previously visited,  $h_{0\phi}$  is the depot node for this tour,  $h_{l\phi}$  is the last added node to tour  $\phi$ , and  $c_\phi$  shows the remaining capacity for tour  $\phi$ . Then, the key and value of the  $i^{th}$  node is defined as:

$$k_i = W^{K_3} h_i, v_i = W^{V_2} h_i \quad (23)$$

and now we compute the compatibility of the query with all nodes as follows:

$$\mu_i = softmax(\frac{q k_i^T}{\sqrt{dim_k}}) v_i \quad (24)$$

To compute the output probabilities for visiting each node, we employ a final layer with a single attention head. In this layer,  $\mu_i$  serves as the query and  $h_i$  as the key. The compatibility scores are calculated and then clipped within the range  $[-A, A]$  (with  $A = 10$ ) using the  $\tanh$  function.

Now, we apply a masking function to enforce the threshold condition outlined in Equation 10 while also handling visited nodes. The log-probabilities of selecting the depot as the next node, which would deactivate an initiated tour, is set to zero if the tour’s current used capacity is below a defined threshold  $\mathcal{T}_t$  by Equation 10 for iteration  $t$ . If the tour’s current capacity exceeds this threshold, the selection of the

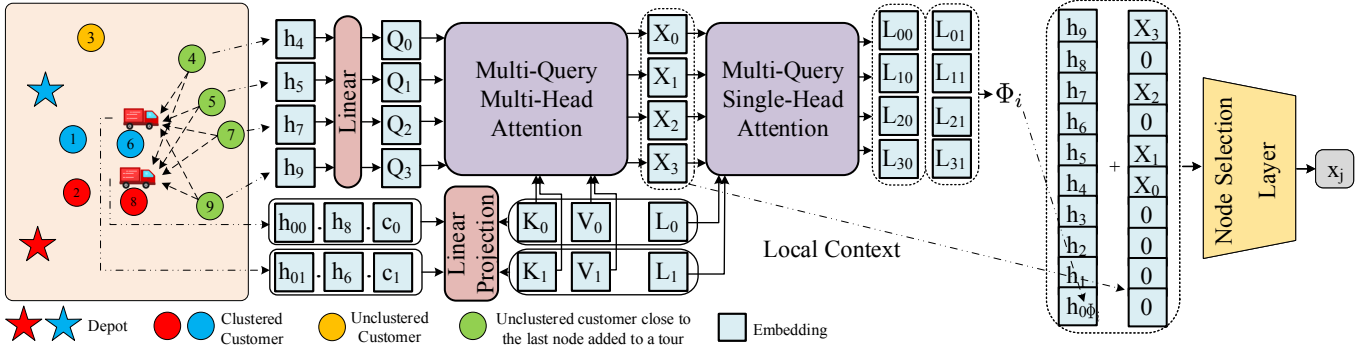


Fig. 2. The architecture of Vehicle Selection and Local Context Generation Layer (VSLCGL). First, the model selects the top  $k = 4$  nearest unvisited customers relative to the last nodes in active tours. The embeddings of these selected customers are passed through a Multi-Query Multi-Head Attention mechanism, where the keys and values are derived from the state of active tours. This state includes the embedding of the tour's origin depot, the embedding of the last visited node, and the tour's current capacity usage. The Multi-Query Multi-Head Attention generates a local context for each selected customer, capturing the dynamic interaction between the customer and the ongoing tour. This context is subsequently refined through a Multi-Query Single-Head Attention mechanism, which produces logits that guide the selection of the most suitable tour for the next node assignment. Finally, the local context is integrated with the initial node embeddings, enabling the Node Selection Layer (NSL) to capture the dynamic interactions between nodes and all active tours. Best viewed in color.

depot becomes conditional on the model's preference. This is formally represented as follows:

$$\mu_i^f = \begin{cases} \mu_0, & \text{if } i = 0 \text{ \& } C_\phi > \mathcal{T}_t, \\ \mu_i, & \text{if } i \neq 0 \text{ \& } i \text{ is not visited,} \\ -\infty, & \text{Otherwise} \end{cases} \quad (25)$$

and finally, the probabilities are defined as:

$$p_i = p_\theta(\pi_t = I_i | s_t) = \text{softmax}(\mu_i^f) \quad (26)$$

#### D. Training algorithm

We adopt the policy gradient with rollout baseline [25] to train the model. We define loss function as  $\mathcal{L}(\theta|s) = \mathbb{E}_{p_\theta(\pi|s)}[L(\pi)]$  and we optimize it using REINFORCE algorithm to estimate policy gradient as follow:

$$\nabla \mathcal{L}(\theta|s) = \mathbb{E}_{p_\theta(\pi|s)}[(L(\pi) - b(s))\nabla \log p_\theta(\pi|s)] \quad (27)$$

The policy network  $\pi_\theta$  generates probability vectors for tours and nodes, selecting one of each at each decoding step. A baseline network with the same architecture is used as a greedy rollout baseline to construct the tours by always selecting tours and nodes with the highest probability. Finally, the reward value is calculated based on the generated tours.

The value of  $\mathcal{L}(\theta|s)$  is determined according to Equation 7 and is calculated as the sum of the negative optimal length of all tours. As calculating tour lengths using traditional heuristics is time-consuming and significantly increases training time, we use a learned TSP model with the same architecture as presented by Kool et al. [25] to approximate the minimum length of each tour [11]. Since the number of customers in each tour may vary by other tours, we use padding by adding the depot node multiple times to ensure all tours have the same number of nodes, enabling parallel calculation of tour length. Each generated tour is then fed into the trained TSP model to obtain the approximate minimum length for each tour. The training algorithm for our model is shown in Algorithm 1.

#### Algorithm 1: Training Algorithm with rollout baseline

```

1 Input: Number of epochs  $E$ , batch size  $B$ , steps  $T$ , trained TSP model  $AM$ 
   Initialize  $\theta = \theta^{BL} = \theta_0$ 
2 for  $epoch = 1, \dots, E$  do
3   for  $step = 1, \dots, T$  do
4     Generate Random instances  $s_i, \forall i \in \{1, \dots, B\}$ 
5     Sample Generate tours using policy  $p_\theta, \forall i \in \{1, \dots, B\}$ 
6     Greedily generate tours using policy  $p_\theta^{BL}, \forall i \in \{1, \dots, B\}$ 
7     Padding all routes of  $\pi_i$  and  $\pi_i^{BL}, \forall i \in \{1, \dots, B\}$ 
8     Calculate the loss  $L(\pi_i), L(\pi_i^{BL})$  using  $AM, \forall i \in \{1, \dots, B\}$ 
9      $\nabla \mathcal{L} \leftarrow \frac{1}{B} \sum_{i=1}^B (L(\pi_i) - L(\pi_i^{BL})) \nabla \log p_\theta(\pi_i)$ 
10     $\theta \leftarrow Adam(\theta, \nabla \mathcal{L})$ 
11  if  $p_\theta$  provides better result than  $p_\theta^{BL}$  then  $\theta^{BL} \leftarrow \theta$ 

```

#### E. Enhancing AM for large-scale MDVRP

We employ the AM [25] in both training and inference phases to determine the minimum travel distances for each tour. Our experiments reveal that while the AM, trained on a uniform distribution, delivers near-optimal solutions for small-scale MDVRP instances, its performance declines as the size of the MDVRP increases – a limitation also evident in the results presented by Hou et al. [11]. This decline is due to the deviation from uniformity in the distribution of customer and depot locations within each tour.

To improve the generalization capability of the AM for generating near-optimal solutions across tours produced by our proposed model, we developed a specialized training procedure. Initially, we trained our method on small-scale MDVRP instances, utilizing an AM pre-trained on 10 nodes with a uniform distribution as the TSP solver. Subsequently, we applied our trained model to a large-scale randomly generated MDVRP dataset and retrained AM using the list of tours generated by the model. To handle the variability in the number of nodes per instance in each batch of data, we implemented a padding technique that repeated the first node (the depot) to ensure a consistent number of nodes across all AM inputs. This retraining significantly enhanced the AM's capability to generate near-optimal paths, not only for large-scale MDVRP but also for very large-scale VRP instances.

## VI. EXPERIMENTAL EVALUATION

### A. Experimental setup

**Hyperparameters:** We follow previous works [10], [25], [41] and sample the coordinates of  $|\mathcal{D}|$  depots and  $|\mathcal{U}|$  customers uniformly from the domain  $[0, 1]$ . The demand for each customer is randomly selected between 1 and 10. The vehicle capacities for instances with 100, 200, 400, 700, and 1,000 customers are set to 50, 100, 150, 175, and 200, respectively. We generate 1,280,000 instances on the fly as training datasets. During the training phase, we use the AM [25], which is trained on 10 nodes, as the path generator for each tour.

We trained our model for 100 epochs with a batch size of 512. However, for training instances with 200 nodes and 3 or 4 depots, we reduced the batch size to 400 due to memory constraints. We choose 6 layers encoder with 8 heads and the default dimension of embedding is 128. The learning rate is constant  $\eta = 10^{-4}$ . All methods are tested on 100 instances for MDVRP with 100, 200, 400, 700, and 1,000 nodes, each on 2, 3, and 4 depots.

**Baselines:** We evaluate our method using two key metrics: objective value as total driving distance and runtime. To ensure robust comparisons, we selected a range of baselines:

- **HGS:** We use Hybrid Genetic Search (HGS) [14] implemented in PyVRP [42] version 0.8.2.
- **OR-tools:** To solve MDVRP instances using OR-tools, we set the PATH\_CHEAPEST\_ARC strategy for the initial solution and GUIDED\_LOCAL\_SEARCH for local search metaheuristics.
- **GA:** We use the Genetic Algorithm [9] for MDVRP with 500 generations with a 0.05 rate for crossover, mutation, and route merging, and a population size of 25.
- **Cluster+AM:** This method involves clustering each instance using the algorithm proposed by Surekha et al. [7] and then solving the single-depot VRP in each cluster using Attention Model (AM) [25].
- **Cluster+POMO:** Using the same clustering strategy, we substitute AM by POMO [41] with 8 augment inference, a state-of-the-art method for combinatorial optimization.
- **Cluster+GLOP (LKH3):** Following the same clustering strategy, we replace AM with GLOP [10], the current state-of-the-art non-autoregressive learning-based CVRP solver, which leverages LKH3 as its TSP solver.
- **GLOP (LKH3):** We modified the GLOP [10] to apply multi-depot. Following the paper, we generated a heatmap for all nodes and constructed tours in a round-robin order, starting from the first depot. After ending a tour, we moved to the next depot, repeating until all customers were served. LKH3 was used to solve the TSP.
- **MADRL:** We adopt the Multi-Agent Deep Reinforcement Learning method for MDVRP [8] and apply 2-opt after a greedy search.

**Inference:** During inference, our trained model partitions the MDVRP instance into several tours. The visiting sequence is determined using either LKH3 in parallel on the CPU or by

utilizing the AM. For instances with 100 customers, we use DeepMDV trained on 100 nodes and the AM trained on 10 nodes. For larger instances, we utilize DeepMDV trained on 200 nodes and the AM trained with the proposed procedure. We also set the value of  $k$  in VSLCGL to 50% of the number of customers for instances of size 100 and 30% of the number of customers for larger instances. We evaluate our method using four different strategies:

- **DeepMDV (AM, G):** This strategy utilizes our proposed method with AM as the pathfinder with greedy search techniques for both partitioning and pathfinding.
- **DeepMDV (LKH3, G):** Here, our method incorporates the LKH3 algorithm for pathfinding, while the partitioning is done using a greedy search approach.
- **DeepMDV (LKH3, G, P):** We utilize multiple GPUs to run the greedy search in parallel with various values of  $k$ —specifically 30%, 40%, 50% and 60% of the number of customers. By incorporating the LKH3 algorithm for pathfinding, we report the average of the best results obtained for each instance.
- **DeepMDV (AM, S):** This strategy applies our proposed method with a greedy search AM for pathfinding and sampling with a size of 1,000 for partitioning model.

**Computational devices:** We trained our model on a single NVIDIA Tesla V100 GPU. Learning-based methods are tested on an NVIDIA Tesla V100 GPU paired with an Intel Xeon Gold 6254 CPU (18 vCores), running Ubuntu 20.04 OS with 175 GB of Memory. Non-learning methods are executed on an AMD EPYC 9474F CPU with 28 vCores, using Ubuntu 20.04 and 110 GB of memory.

### B. Results of MDVRP on large-scale synthetic dataset

We report the average testing results on 100 random instances in Table I for  $|\mathcal{D}| = 2, 3$ , and 4. HGS consistently delivers the best results for MDVRP instances with up to 400 customers within the allocated time. However, its computational demands grow significantly as problem size increases, requiring substantially more time to remain effective. Similarly, while GA performs well on small-scale instances, its efficiency declines sharply with larger datasets. For instances exceeding 400 customers, GA encounters memory constraints and excessive computational time, rendering it unable to produce viable solutions within practical limits.

Clustering with AM and POMO performs well for smaller instances, while clustering with GLOP demonstrates better scalability for larger ones. Although cluster-based POMO excels on small-scale problems, it faces challenges with larger instances, similar to AM. For CVRP100 scenarios, POMO outperforms MADRL in cases with two and three depots, but our method surpasses POMO in all scenarios using LKH3. For larger problem instances, DeepMDV (AM, G) consistently outperforms POMO, delivering superior results.

The results from GLOP (LKH3), which employs a round-robin approach for selecting each depot as a starting point, show that this method fails to deliver high-quality solutions.

TABLE I

PROPOSED METHOD VS BASELINES ON A SYNTHETIC DATASET. THE OBJECTIVE (OBJ.) REPRESENTS THE DRIVING DISTANCE, AND THE PERCENTAGE GAP (G) IS RELATIVE TO THE HGS. THE BEST VALUE ACROSS ALL METHODS IS MARKED BY (\*). RUN TIMES ARE REPORTED IN THE COLUMN LABELED (T). FOR A FAIR COMPARISON WITH TRADITIONAL METHODS, ALL APPROACHES, SOLVE EACH INSTANCE ONE BY ONE, AND WE REPORT THE AVERAGE RUNTIME PER INSTANCE. THE BEST RESULTS ACROSS ALL METHODS, EXCLUDING HGS, ARE HIGHLIGHTED IN BOLD.

Methods	D	CVRP100			CVRP200			CVRP400			CVRP700			CVRP1k		
		Obj.	G(%)	T(s)	Obj.	G(%)	T(s)	Obj.	G(%)	T(s)	Obj.	G(%)	T(s)	Obj.	G(%)	T(s)
HGS	2	13.01*	0.00	20	15.5*	0.00	30	21.6*	0.00	40	31.85	0.00	50	40.12	0.00	60
OR-tools		13.8	6.07	60	16.5	6.45	240	23.4	8.33	480	33.26	4.42	720	40.77	1.62	960
GA		14.01	7.68	21	18.19	17.35	110	27.01	25.0	540	-	-	-	-	-	-
Cluster + AM (bs30)		13.98	7.45	0.2	17.44	12.5	0.3	25.9	19.9	0.55	39.24	23.2	1	54.1	34.8	1.4
Cluster + POMO		13.78	5.91	0.2	16.36	5.54	0.3	23.8	10.2	0.7	37.1	16.5	1.2	54.6	36.1	1.7
Cluster + GLOP (LKH3)		15.8	21.4	0.35	18.9	21.9	0.7	24.3	12.5	1	33.2	4.23	1.8	40.06	-0.14	2.7
GLOP (LKH3)		32.02	246	0.35	40.64	262	0.6	63.53	294	0.8	98.5	315	1.3	134	346	2
MADRL		13.93	7.07	1.7	17.24	11.2	2.8	24.8	14.8	4.6	37.4	17.4	7.2	50.3	25.4	9.2
DeepMDV (AM, G)		13.84	6.37	0.45	16.52	6.58	0.8	22.76	5.37	1.7	32.1	0.78	2.9	39.76	-0.9	4.1
DeepMDV (LKH3, G)		13.78	5.91	1	16.30	5.16	1.5	22.36	3.51	2.4	31.56	-0.91	3.9	39.03	-2.71	5.6
DeepMDV (LKH3, G, P)		13.59	4.45	1	16.08	3.74	1.5	<b>22.07</b>	<b>2.17</b>	2.4	<b>31.2*</b>	<b>-2.04</b>	3.9	<b>38.67*</b>	<b>-3.61</b>	5.6
DeepMDV (AM, S)		<b>13.34</b>	<b>2.53</b>	1.1	<b>16.02</b>	<b>3.35</b>	2.6	22.25	3.00	8.2	-	-	-	-	-	-
HGS	3	11.87*	0.00	20	14.32*	0.00	30	20.74*	0.00	40	29.79	0.00	50	37.51	0.00	60
OR-tools		12.66	6.65	60	15.54	8.51	240	22.05	6.31	480	31.15	4.56	720	38.19	1.81	960
GA		12.88	8.50	18	16.95	18.4	108	25.88	24.8	504	-	-	-	-	-	-
Cluster + AM (bs30)		13.15	10.8	0.2	16.77	17.1	0.3	25.11	21.1	0.55	37.6	26.2	1	50.73	35.2	1.4
Cluster + POMO		12.91	8.76	0.2	15.87	10.8	0.3	21.96	5.88	0.7	33.0	10.8	1.2	45.0	19.9	1.7
Cluster + GLOP (LKH3)		15.02	26.5	0.35	17.3	21.4	0.75	23.03	11.0	1	31.1	4.39	1.8	37.58	0.18	2.6
GLOP (LKH3)		31.53	265	0.35	40.8	284	0.6	64.05	308	0.8	101.2	339	1.3	133.7	356	2
MADRL		12.96	9.18	1.8	16.31	13.9	3	23.84	14.9	4.7	35.9	20.5	7.4	47.5	26.6	9.5
DeepMDV (AM, G)		12.82	8.00	0.46	15.61	9.00	0.9	21.58	4.05	1.7	30.23	1.47	2.9	37.44	-0.18	4.2
DeepMDV (LKH3, G)		12.76	7.49	1	15.36	7.26	1.5	21.18	2.12	2.4	29.64	-0.5	3.9	36.64	-2.31	5.7
DeepMDV (LKH3, G, P)		12.57	5.89	1	15.08	5.3	1.5	<b>20.94</b>	<b>0.96</b>	2.4	<b>29.35*</b>	<b>-1.47</b>	3.9	<b>36.29*</b>	<b>-3.25</b>	5.7
DeepMDV (AM, S)		<b>12.23</b>	<b>3.03</b>	1.3	<b>15.03</b>	<b>4.95</b>	3.4	20.97	1.1	10.4	-	-	-	-	-	-
HGS	4	11.06*	0.00	20	13.61*	0.00	30	19.9*	0.28	40	28.45	0.00	50	36.33	0.00	60
OR-tools		11.8	6.69	60	14.64	7.56	240	20.97	5.37	480	29.66	4.25	720	36.21	-0.33	960
GA		12.09	9.31	17	16.01	17.6	106	23.92	20.2	468	-	-	-	-	-	-
Cluster + AM (bs30)		12.54	13.3	0.2	16.72	22.8	0.3	25.08	26.0	0.55	37.68	32.4	1	50.4	38.7	1.4
Cluster + POMO		12.07	9.13	0.2	15.62	14.7	0.3	21.15	6.28	0.7	30.44	6.99	1.2	39.9	9.82	1.7
Cluster + GLOP (LKH3)		14.44	30.6	0.45	17.23	26.6	0.8	22.38	12.4	1	29.76	4.6	1.8	36.64	0.85	2.6
GLOP (LKH3)		31.35	283	0.35	40.72	299	0.6	63.61	319	0.8	99.8	350	1.3	134	368	2
MADRL		12.05	8.95	1.9	15.71	15.4	3	23.02	15.7	4.9	35.15	23.5	7.6	45.9	26.3	9.7
DeepMDV (AM, G)		11.95	8.04	0.47	15.07	10.7	0.9	20.93	5.17	1.7	29.43	3.44	3	36.48	0.41	4.2
DeepMDV (LKH3, G)		11.89	7.5	1	14.83	8.96	1.5	20.49	2.96	2.4	28.77	1.12	3.9	35.64	-1.89	5.7
DeepMDV (LKH3, G, P)		11.73	6.05	1	14.58	7.12	1.5	<b>20.18</b>	<b>1.4</b>	2.4	<b>28.37*</b>	<b>-0.28</b>	3.9	<b>35.13*</b>	<b>-3.3</b>	5.7
DeepMDV (AM, S)		<b>11.47</b>	<b>3.7</b>	1.5	<b>14.38</b>	<b>5.65</b>	3.9	20.25	1.75	12.7	-	-	-	-	-	-

It also highlights that single-depot VRP approaches are not directly applicable to the MDVRP using this strategy.

The MADRL method produces high-quality solutions for smaller instances but struggles to generalize to instances exceeding 200 nodes. Across all problem sizes and depot configurations, our method, even when utilizing a simple greedy search strategy, consistently outperforms MADRL in both solution quality and computational efficiency.

Our method, using a greedy search, outperforms clustering-based algorithms. DeepMDV which uses greedy search and runs four parallel instances with varying values of  $k$  for each problem instance, provides higher-quality solutions while maintaining a comparable runtime. This approach yields up to a 1.5% improvement over using a single instance with a predefined value for  $k$ . However, achieving this performance requires running the model on multiple GPUs, as executing multiple instances on the same GPU may reduce its efficiency

and increase the algorithm's runtime.

Our findings reveal that DeepMDV, when employing a sampling strategy, delivers superior results compared to greedy search, albeit with increased computational time. For problem instances with more than 700 customers, we exclude sampling results due to its runtime exceeding 10 seconds. In CVRP100, for scenarios with two, three, and four depots, DeepMDV with sampling achieves gaps of 2.53%, 3.03%, and 3.7%, respectively, relative to the best solutions provided by HGS.

### C. Performance on spatially skewed customers

To further assess the proposed method, we created another synthetic dataset where the customer locations follow a skewed distribution — densely clustered in one region, with depots positioned at a distance. This setup mimics real-world logistics scenarios where major hubs like airports or seaports serve as depots. Instances were constructed with fixed depot locations

TABLE II

EMPIRICAL RESULTS FOR INSTANCES WITH SPATIALLY SKEWED CUSTOMER LOCATIONS GENERATED BY BETA AND GAMMA DISTRIBUTION. THE OBJECTIVE (OBJ.) REPRESENTS THE DRIVING DISTANCE, AND THE PERCENTAGE GAP (G) IS RELATIVE TO THE HGS. THE BEST VALUE AMONG ALL METHODS IS MARKED WITH (\*), WHILE THE BEST RESULTS EXCLUDING HGS ARE HIGHLIGHTED IN BOLD.

Methods	D	Beta Distribution									Gamma Distribution								
		CVRP100			CVRP400			CVRP1k			CVRP100			CVRP400			CVRP1k		
		Obj.	G(%)	T(s)	Obj.	G(%)	T(s)	Obj.	G(%)	T(s)	Obj.	G(%)	T(s)	Obj.	G(%)	T(s)	Obj.	G(%)	T(s)
HGS	2	17.1*	0.00	20	25.8*	0.00	60	45.9*	0.00	180	18.7*	0.00	20	28.0*	0.00	60	49.6*	0.00	180
Cluster + AM (bs30)		18.2	6.43	0.2	30.5	18.2	0.6	57.5	25.3	1.4	19.9	6.41	0.2	33.4	19.3	0.6	72.1	45.4	1.4
Cluster + POMO		18.0	5.26	0.2	26.5	2.71	0.7	52.1	13.5	1.7	19.6	4.81	0.2	29.8	6.42	0.7	58.4	17.7	1.7
Cluster + GLOP		19.2	12.3	0.3	27.2	5.42	1	48.6	5.9	2.7	21.5	15.0	0.3	30.6	9.28	1	54.5	9.87	2.7
MADRL		18.2	6.43	1.7	29.4	14.0	4.6	53.8	17.2	9.2	19.8	5.88	1.7	32.5	16.1	4.6	59.8	20.6	9.2
DeepMDV (AM, G)		18.1	5.84	0.4	27.1	5.03	1.7	48.7	6.1	4.1	19.5	4.27	0.4	29.0	3.57	1.7	51.9	4.63	4.1
DeepMDV (LKH3, G)		17.9	4.67	1	26.5	2.71	2.4	47.7	3.92	5.6	19.3	3.2	1	28.5	1.78	2.4	50.8	2.41	5.6
DeepMDV (LKH3, G, P)		<b>17.7</b>	<b>3.5</b>	1	<b>26.3</b>	<b>1.93</b>	2.4	<b>47.2</b>	<b>2.83</b>	5.6	<b>19.2</b>	<b>2.67</b>	1	<b>28.3</b>	<b>1.07</b>	2.4	<b>50.5</b>	<b>1.81</b>	5.6
HGS	3	15.2*	0.00	20	23.1*	0.00	60	40.6*	0.00	180	17.8*	0.00	20	26.5*	0.00	60	47.9*	0.00	180
Cluster + AM (bs30)		16.6	9.21	0.2	27.6	19.5	0.6	52.7	29.8	1.4	19.6	10.1	0.2	32.1	21.1	0.6	59.2	23.6	1.4
Cluster + POMO		16.3	7.23	0.2	24.7	6.92	0.7	49.8	22.7	1.7	19.2	7.86	0.2	28.4	7.16	0.7	56.5	17.8	1.7
Cluster + GLOP		18.2	19.7	0.4	26.3	13.9	1	45.9	13.1	2.6	20.4	14.6	0.4	29.3	10.6	1	52.4	9.39	2.6
MADRL		16.3	7.23	1.8	26.8	16.0	4.7	51.1	25.9	9.5	19.2	7.86	1.8	31.3	18.1	4.7	58.3	21.1	9.5
DeepMDV (AM, G)		16.2	6.57	0.4	25.3	9.52	1.7	45.4	11.8	4.2	18.5	3.93	0.4	27.8	4.90	1.7	50.5	5.42	4.2
DeepMDV (LKH3, G)		16.0	5.26	1	24.8	7.35	2.4	44.1	8.62	5.7	18.3	2.80	1	27.4	3.39	2.4	49.3	2.92	5.7
DeepMDV (LKH3, G, P)		<b>15.8</b>	<b>3.94</b>	1	<b>24.5</b>	<b>6.06</b>	2.4	<b>43.2</b>	<b>6.40</b>	5.7	<b>18.2</b>	<b>2.24</b>	1	<b>27.2</b>	<b>2.64</b>	2.4	<b>49.0</b>	<b>2.29</b>	5.7
HGS	4	15.1*	0.00	20	22.4*	0.00	60	39.8*	0.00	180	17.3*	0.00	20	25.8*	0.00	60	46.5*	0.00	180
Cluster + AM (bs30)		17.1	13.2	0.2	28.3	26.3	0.6	56.4	41.7	1.4	19.2	11.0	0.2	34.4	33.3	0.6	61.4	32.0	1.4
Cluster + POMO		16.4	8.61	0.2	25.4	13.4	0.7	47.3	18.8	1.7	19.7	13.9	0.2	28.6	10.9	0.7	55.7	19.8	1.7
Cluster + GLOP		18.1	19.9	0.4	25.7	14.7	1	45.2	13.56	2.6	20.1	16.2	0.4	29.1	12.8	1	52.1	12.0	2.6
MADRL		16.7	10.6	1.9	27.6	23.2	4.8	53.2	33.7	9.7	18.7	8.09	1.9	30.6	18.6	4.8	56.4	21.2	9.7
DeepMDV (AM, G)		15.8	4.63	0.4	24.3	8.48	1.7	43.1	8.29	4.2	18.0	4.04	0.4	26.7	3.48	1.7	49.2	5.80	4.2
DeepMDV (LKH3, G)		15.7	3.97	1	23.8	6.25	2.4	42.0	5.52	5.7	17.8	2.89	1	26.4	2.32	2.4	48.2	3.65	5.7
DeepMDV (LKH3, G, P)		<b>15.6</b>	<b>3.31</b>	1	<b>23.6</b>	<b>5.35</b>	2.4	<b>41.6</b>	<b>4.52</b>	5.7	<b>17.7</b>	<b>2.31</b>	1	<b>26.2</b>	<b>1.55</b>	2.4	<b>47.9</b>	<b>3.01</b>	5.7

for: i) two depots:  $\{[0, 1], [1, 1]\}$ , ii) three depots:  $\{[0, 1], [0.5, 1], [1, 1]\}$ , iii) four depots:  $\{[0, 1], [0.33, 1], [0.66, 1], [1, 1]\}$ . Customer locations were generated using a beta distribution ( $\mu = 3, \sigma = 1$ ) and a gamma distribution (shape  $k = 7$ , scale  $\theta = 1$ ), normalized to the range  $[0, 1]$ . To ensure fair evaluation, we used the pre-trained model and retrained DeepMDV along with all learning-based baselines on these dataset for a single epoch. We set the number of nearest neighbors in VSLCGL to 60% of the number of customers.

By skewing customer locations, we test the model's ability to recognize and exploit the benefits of assigning customers to the most suitable depot, even if it involves a greater initial distance, thereby optimizing overall efficiency. Results are summarized in Table II. Heuristic-based methods face significant challenges in delivering high-quality solutions under such skewed conditions. To address this limitation, we extended the running time of HGS, increasing it from 30 seconds to 40 seconds for smaller instances and from 60 seconds to 180 seconds for larger ones, allowing the algorithm more time to produce competitive results.

As anticipated, the clustering-then-routing approach performed poorly in this setting. Its reliance on proximity to depots led to suboptimal routes with underutilized vehicle capacities from certain depots. In contrast, DeepMDV demonstrated substantially better performance. Notably, while the performance gap between DeepMDV (LKH3, G) and GLOP

for normally distributed customer locations was less than 4% in CVRP1k, this gap widened to over 8% in the skewed scenario. These results highlight the robustness of DeepMDV, demonstrating that it consistently outperforms baseline methods by optimizing the entire problem holistically.

#### D. Results on a real world dataset

To further evaluate the effectiveness of the DeepMDV, we tested it against state-of-the-art solution on a real-world MDVRP dataset. This dataset includes multiple MDVRP instances, with scenarios involving up to 9 depots and several hundred customers. For our experiments, we selected instances with 2-4 depots, excluding those with additional constraints such as delivery time windows. The selected instances are from notable sources: p01, p02, p04, p05, p06, and p07 were first introduced by Christofides et al. [43], while p12 and p15 were detailed by Chao et al. [44]. The results of various methods on this dataset are presented in Table III.

On average, MADRL exhibits a 10.28% deviation from the optimal value across all instances. In contrast, DeepMDV, utilizing a greedy search, delivers solutions in under 1 second, with an average gap of 8.89%. With additional time and employing a sampling search, DeepMDV can further reduce this gap to 5.97% of the optimal solutions, still achieving results in less than 2 seconds per instance.

TABLE III

PROPOSED METHOD VS MADRL ON REAL MDVRP INSTANCES. THE OBJECTIVE (OBJ.) REPRESENTS THE DRIVING DISTANCE, AND THE PERCENTAGE GAP (G) IS W.R.T. THE OPTIMAL OR KNOWN UPPER BOUND FOR THE INSTANCES. RUN TIMES ARE REPORTED IN THE COLUMN LABELED (T). ALL METHODS SOLVE EACH PROBLEM INSTANCE SEQUENTIALLY. FOR ALL INSTANCES,  $k = 50\%$  OF THE NUMBER OF CUSTOMERS.

Instance	Scale	$ \mathcal{D} $	MADRL		DeepMDV (AM, G)		DeepMDV (LKH3, G)		DeepMDV (AM, S)	
			G(%)	T(s)	G(%)	T(s)	G(%)	T(s)	G(%)	T(s)
p04	102	2	9.06	< 2	8.29	< 1	8.09	< 2	<b>4.96</b>	< 2
p05	102	2	8.32	< 2	8.78	< 1	5.72	< 2	<b>4.59</b>	< 2
p12	82	2	10.34	< 2	10.39	< 1	10.08	< 1	<b>6.75</b>	< 2
p06	103	3	9.32	< 2	8.14	< 1	7.33	< 2	<b>5.53</b>	< 2
p01	54	4	7.22	< 1	7.68	< 1	7.52	< 1	<b>5.44</b>	< 2
p02	54	4	10.67	< 1	8.69	< 1	8.52	< 1	<b>4.89</b>	< 2
p07	104	4	9.41	< 2	7.42	< 1	7.06	< 2	<b>4.82</b>	< 2
p15	164	4	17.94	< 2	17.4	< 1	16.83	< 2	<b>10.81</b>	< 2
Average	-	-	10.28	< 2	9.59	< 1	8.89	< 2	<b>5.97</b>	< 2

## VII. EXTENDED EVALUATIONS

### A. Sensitivity analysis

To assess the impact of different numbers of neighboring customers selected for generating local context on solution quality, we tested DeepMDV with different values of  $k$ . We define the best value for each problem instance as the minimum value obtained across all runs with different  $k$  values. The average results across 100 problem instances, compared to the average of the best solutions, are presented in Figure 3.

While smaller  $k$  values leads to suboptimal solutions across all tested distributions, each instance stabilizes after reaching a specific threshold. Beyond this point, increasing  $k$  only adds computational overhead without affecting solution quality. For large instances with uniform distributions, setting  $k$  to 30% of the total customers delivers strong performance. However, a  $k$ -value of 50% consistently yields high-quality solutions across all tested distributions and customer counts, making it a promising choice for balancing efficiency and effectiveness.

### B. Generalizability

Our method demonstrates strong generalizability beyond just varying the number of customers and it effectively solves MDVRP instances with different numbers of depots than those used during training. This makes it equally well-suited for single-depot VRP problems. Table VII-B presents the results of our proposed method, trained on MDVRP with two depots, compared against baselines specifically designed and trained for single-depot VRPs on 100 instances of the VRP problem.

As shown in the table, our method, utilizing LKH3 as the pathfinder, outperforms all baselines in instances with more than 200 customers. Additionally, our method surpasses GLOP, the state-of-the-art VRP solver, for CVRP7k by approximately 1.54%. Moreover, running multiple instances of our method in parallel with different values of  $k$  further enhances the results. By running five instances with  $k$  values set to 200, 300, 400, and 500 for CVRP1k, CVRP2k, and CVRP7k, our method consistently outperforms GLOP by at least 2.45%, 2.1%, and 2.3%, respectively.

We further evaluate the generalizability of our method in scenarios where the number of depots used during training differs from those in testing, with the results presented in

Table V. As expected, the model performs best when the number of depots in training and testing matches. However, our model also demonstrates strong adaptability; it can still deliver high-quality solutions for instances with fewer depots than those used during training. For instance, the model trained on MDVRP with three depots performs comparably to the one trained on two depots when applied to MDVRP100 instances with three depots. This trend holds true for MDVRP100 instances with three and four depots as well.

DeepMDV trained on three depots exhibits strong performance across scenarios with both fewer and greater numbers of depots. For MDVRP100, this model achieves gaps of 0.61%, 0%, and 1.68% for instances with one, two, and four depots, respectively, compared to the MDVRP trained on the same number of depots. Similarly, for MDVRP1000, the gaps are 1.11%, 1.28%, and 1.12%, respectively.

### C. Ablation study

**AM trained with new approach VS on uniform distribution:** Our analysis shows that for MDVRP with two depots and 100 customers, the performance gap between the AM trained on a uniform distribution and LKH3 is under 0.5%. However, as problem size increases to 200, 400, 700, and 1000 customers, this gap grows to 4.35%, 9.5%, 15.7%, and 19.3%, respectively. Training the AM with our proposed approach reduces these gaps to 1.34%, 1.78%, 1.71%, and 1.87%, respectively. This demonstrates that our training method significantly improves solution quality for larger instances, making it advantageous for models relying on AM as a secondary solver in large-scale problems.

**Components in the proposed method:** We conduct ablation studies to evaluate the impact of key components in our method: Local Context summation with the embedding (LC), the optimal number of tours (ONT), and coordinate transformation (CT). For each study, we retrain the model without one component while maintaining all other configurations. This allows us to isolate and quantify each component's contribution to performance. The results presented in Table VI for MDVRP instances with 100 and 1000 customers and two depots validate the efficacy of each component's design.

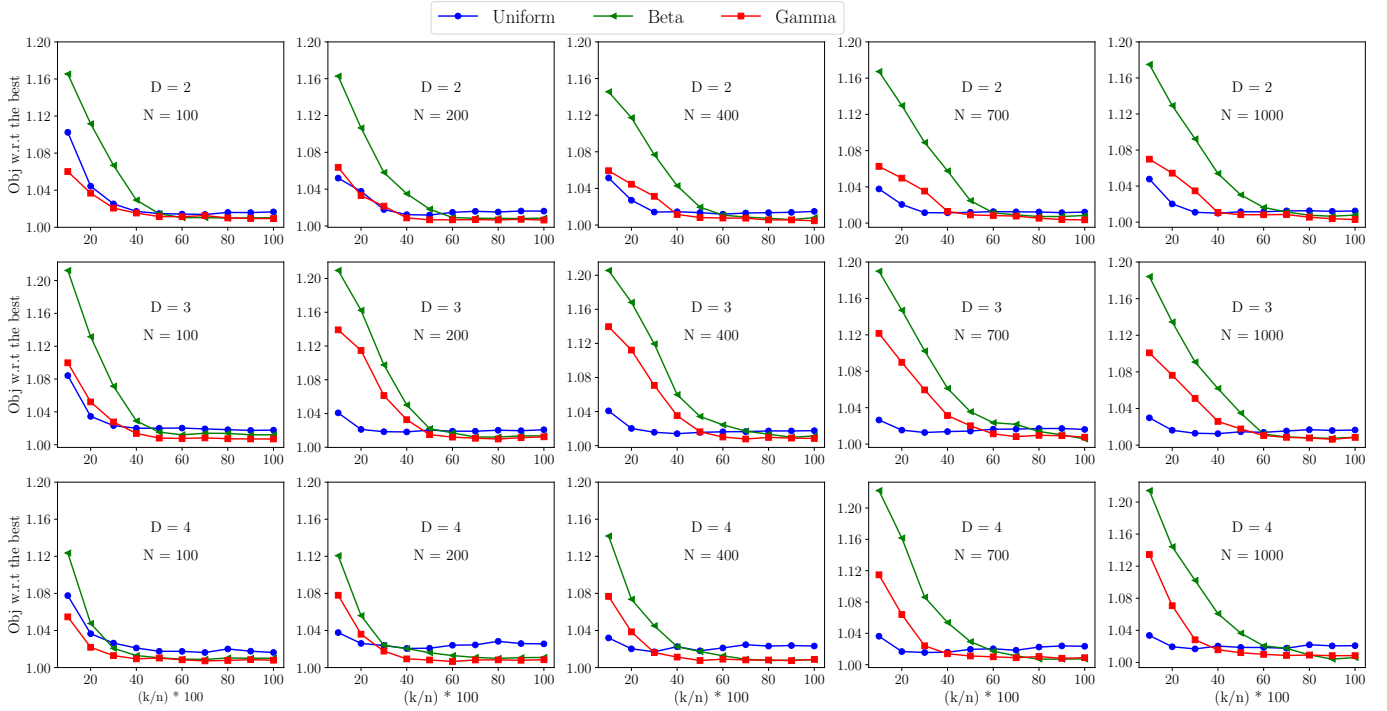


Fig. 3. Sensitivity analysis of the influence of  $k$  on solution quality, run on a synthetic dataset. The X-axis displays the value of  $k$  as a percentage of the problem size, while the Y-axis represents the average cost relative to the best value achieved by the model. The best values are calculated as the average of the minimum costs for each instance in the dataset, evaluated for different values of  $k$ .

TABLE IV

PERFORMANCE OF PROPOSED METHOD TRAINED ON MDVRP WITH TWO DEPOTS VS BASELINES FOR SINGLE DEPOT VRP. THE OBJECTIVE (OBJ.)

REPRESENTS THE DRIVING DISTANCE, AND THE PERCENTAGE GAP (G) IS RELATIVE TO THE HGS. THE BEST VALUE ACROSS ALL METHODS, MARKED BY (\*). RUN TIMES ARE REPORTED IN THE COLUMN LABELED (T). ALL METHODS SOLVE EACH PROBLEM INSTANCE SEQUENTIALLY, AND WE REPORT THE AVERAGE RUNTIME PER INSTANCE. THE BEST RESULTS ACROSS ALL METHODS, EXCLUDING HGS, ARE HIGHLIGHTED IN BOLD.

Methods	CVRP100			CVRP200			CVRP400			CVRP700			CVRP1k		
	Obj.	G(%)	T(s)	Obj.	G(%)	T(s)	Obj.	G(%)	T(s)	Obj.	G(%)	T(s)	Obj.	G(%)	T(s)
HGS	15.5*	0.00	20	17.7*	0.00	40	24.5*	0.00	60	35.2*	0.00	120	43.5*	0.00	180
AM (bs30)	16.4	5.8	0.1	19.6	10.7	0.3	29.3	20.1	0.4	44.2	25.6	1	61.4	42.5	0.8
POMO	<b>15.7</b>	<b>1.29</b>	0.1	18.7	5.64	0.3	29.9	22.0	0.6	47.3	34.4	0.9	101	232	1.2
TAM-AM <sup>†</sup>	16.2	4.51	0.1	-	-	-	27.0	10.2	0.3	-	-	-	50.1	15.2	0.8
TAM-LKH3 <sup>†</sup>	16.1	3.87	0.9	-	-	-	25.9	5.71	1.4	-	-	-	46.3	6.43	1.8
GLOP-LKH3	21.3	20.5	0.3	20.6	16.4	0.7	27.3	11.4	1	38.2	8.52	1.4	45.9	5.51	1.6
DeepMDV (AM, G)	16.3	5.16	0.4	18.9	6.77	0.8	25.7	4.89	1.6	36.8	4.54	2.8	45.5	4.59	3.9
DeepMDV (LKH3, G)	16.2	4.51	0.9	18.7	5.64	1.5	25.4	3.67	2.4	36.3	3.12	3.9	45.0	3.44	5.6
DeepMDV (LKH3, G, P)	16.1	3.87	1	<b>18.5</b>	<b>4.51</b>	1.5	<b>25.3</b>	<b>3.26</b>	2.4	<b>36.0</b>	<b>2.27</b>	3.9	<b>44.8</b>	<b>2.98</b>	5.6

<sup>†</sup> Due to the unavailability of the source code, the results rely on findings from the original literature, resulting in some missing data.

TABLE V

PERFORMANCE OF THE PROPOSED METHOD TRAINED ON DIFFERENT NUMBERS OF DEPOTS ON INSTANCES WITH VARIOUS DEPOT NUMBERS ON A SYNTHETIC DATASET. THE OBJECTIVE (OBJ.) REPRESENTS THE DRIVING DISTANCE, AND THE PERCENTAGE GAP (G) IS RELATIVE TO THE BEST VALUE ACROSS ALL METHODS, MARKED BY (\*).

Methods	CVRP100		CVRP1k		CVRP100		CVRP1k		CVRP100		CVRP1k		CVRP100		CVRP1k	
	Obj.	G(%)	Obj.	G(%)	Obj.	G(%)	Obj.	G(%)	Obj.	G(%)	Obj.	G(%)	Obj.	G(%)	Obj.	G(%)
Trained on $ \mathcal{D} =2$	16.2*	0.00	45.0*	0.00	13.8*	0.00	39.0*	0.00	14.7	14.8	39.2	7.1	15.1	26.9	39.8	11.8
Trained on $ \mathcal{D} =3$	16.3	0.61	45.5	1.11	13.8*	0.00	39.5	1.28	12.8*	0.00	36.6*	0.00	12.1	1.68	36.0	1.12
Trained on $ \mathcal{D} =4$	16.5	1.85	46.2	2.66	13.9	0.72	40.4	3.58	12.8*	0.00	37.4	2.18	11.9*	0.00	35.6*	0.00

## VIII. CONCLUSION

In this paper, we introduce DeepMDV, a deep-learning approach to address the Multi-depot Vehicle Routing Problem (MDVRP). Using an attention mechanism and a two-layer

decoding strategy, DeepMDV first identifies the most suitable tour for assigning the next customer, then selects the optimal customer for that tour. Extensive experiments on synthetic and real-world datasets demonstrate that DeepMDV outperforms existing learning-based methods and integrated VRP ap-

TABLE VI  
EMPRICAL RESULTS OF ABLATION STUDY. THE GAP % IS W.R.T. THE  
RESULTS WITH ALL COMPONENTS IN USE.

CVRP100	CVRP1000	LC	ONT	CT
1.17%	2.9%	×		
0.57%	1.08%		×	
0.72%	2.61%			×

proaches, delivering high-quality solutions for instances with thousands of customers and multiple depots. We also assess all methods on MDVRP instances with spatially skewed customer distributions, demonstrating that DeepMDV delivers markedly superior performance. A thorough analysis further reveals that our method’s generalizability extends beyond the number of customers, handling instances with different numbers of depots than those used during training. The experiments highlight our model’s superiority over state-of-the-art solutions for single-depot VRP, even in instances involving up to 7,000 customers.

## REFERENCES

- [1] H. Wen, Y. Lin, F. Wu, H. Wan, S. Guo, L. Wu, C. Song, and Y. Xu, “Package pick-up route prediction via modeling couriers’ spatial-temporal behaviors,” in *2021 IEEE 37th International Conference on Data Engineering (ICDE)*. IEEE, 2021, pp. 2141–2146.
- [2] E.-C. Blueprint, “In NY daily news: Manhattan bp calls for delivery reforms as nyc residents, businesses receive more than 2.4 million packages per day,” <https://www.manhattanbp.nyc.gov/in-ny-daily-news-manhattan-bp-calls-for-delivery-reforms-as-nyc-residents-businesses-receive-more-than-2-4-million-packages-per-day>, 2022.
- [3] U. S. D. of Energy, “Average annual vehicle miles traveled by major vehicle category,” <https://afdc.energy.gov/data/10309>, 2024.
- [4] Y. Zeng, Y. Tong, and L. Chen, “Last-mile delivery made practical: An efficient route planning framework with theoretical guarantees,” *Proceedings of the VLDB Endowment*, vol. 13, no. 3, pp. 320–333, 2019.
- [5] W. Lyu, H. Wang, Z. Hong, G. Wang, Y. Yang, Y. Liu, and D. Zhang, “REDE: Exploring relay transportation for efficient last-mile delivery,” in *2023 IEEE 39th International Conference on Data Engineering (ICDE)*. IEEE, 2023, pp. 3003–3016.
- [6] W. Ho, G. T. Ho, P. Ji, and H. C. Lau, “A hybrid genetic algorithm for the multi-depot vehicle routing problem,” *Engineering Applications of Artificial Intelligence*, vol. 21, no. 4, pp. 548–557, 2008.
- [7] P. Surekha and S. Sumathi, “Solution to multi-depot vehicle routing problem using genetic algorithms,” *World Applied Programming*, vol. 1, no. 3, pp. 118–131, 2011.
- [8] A. Arishi and K. Krishnan, “A multi-agent deep reinforcement learning approach for solving the multi-depot vehicle routing problem,” *Journal of Management Analytics*, vol. 10, no. 3, pp. 493–515, 2023.
- [9] B. Ombuki-Berman and F. T. Hanshar, “Using genetic algorithms for multi-depot vehicle routing,” in *Bio-inspired Algorithms for the Vehicle Routing Problem*, 2009, pp. 77–99.
- [10] H. Ye, J. Wang, H. Liang, Z. Cao, Y. Li, and F. Li, “GLOP: Learning global partition and local construction for solving large-scale routing problems in real-time,” in *Proceedings of the AAAI Conference on Artificial Intelligence*, vol. 38, no. 18, 2024, pp. 20 284–20 292.
- [11] Q. Hou, J. Yang, Y. Su, X. Wang, and Y. Deng, “Generalize learned heuristics to solve large-scale vehicle routing problems in real-time,” in *The Eleventh International Conference on Learning Representations*, 2022.
- [12] C. Gao, H. Shang, K. Xue, D. Li, and C. Qian, “Towards generalizable neural solvers for vehicle routing problems via ensemble with transferable local policy,” in *Proceedings of the Thirty-Third International Joint Conference on Artificial Intelligence (IJCAI-24)*, 2024.
- [13] P. Toth and D. Vigo, *The vehicle routing problem*. SIAM, 2002.
- [14] T. Vidal, “Hybrid genetic search for the cvrp: Open-source implementation and swap\* neighborhood,” *Computers & Operations Research*, vol. 140, p. 105643, 2022.
- [15] K. Helsgaun, “An extension of the lin-kernighan-helsgaun tsp solver for constrained traveling salesman and vehicle routing problems,” *Roskilde: Roskilde University*, vol. 12, pp. 966–980, 2017.
- [16] M. Alinaghian and N. Shokouhi, “Multi-depot multi-compartment vehicle routing problem, solved by a hybrid adaptive large neighborhood search,” *Omega*, vol. 76, pp. 85–99, 2018.
- [17] M. Wen, W. Sun, Y. Yu, J. Tang, and K. Ikou, “An adaptive large neighborhood search for the larger-scale multi depot green vehicle routing problem with time windows,” *Journal of Cleaner Production*, vol. 374, p. 133916, 2022.
- [18] S. Wang, W. Sun, and M. Huang, “An adaptive large neighborhood search for the multi-depot dynamic vehicle routing problem with time windows,” *Computers & Industrial Engineering*, vol. 191, p. 110122, 2024.
- [19] B. Yu, Z. Yang, and J.-X. Xie, “A parallel improved ant colony optimization for multi-depot vehicle routing problem,” *Journal of the Operational Research Society*, vol. 62, no. 1, pp. 183–188, 2011.
- [20] P. Stodola, “Hybrid ant colony optimization algorithm applied to the multi-depot vehicle routing problem,” *Natural Computing*, vol. 19, no. 2, pp. 463–475, 2020.
- [21] D. Pisinger and S. Ropke, “Large neighborhood search,” *Handbook of Metaheuristics*, pp. 99–127, 2019.
- [22] J. Renaud, G. Laporte, and F. F. Boctor, “A tabu search heuristic for the multi-depot vehicle routing problem,” *Computers & Operations Research*, vol. 23, no. 3, pp. 229–235, 1996.
- [23] A. Paul, R. S. Kumar, C. Rout, and A. Goswami, “Designing a multi-depot multi-period vehicle routing problem with time window: hybridization of tabu search and variable neighbourhood search algorithm,” *Sādhanā*, vol. 46, no. 3, p. 183, 2021.
- [24] B. L. Golden, S. Raghavan, and E. A. Wasil, *The vehicle routing problem: latest advances and new challenges*. Springer Science & Business Media, 2008, vol. 43.
- [25] W. Kool, H. van Hoof, and M. Welling, “Attention, learn to solve routing problems!” in *International Conference on Learning Representations*, 2018.
- [26] C. Contardo and R. Martinelli, “A new exact algorithm for the multi-depot vehicle routing problem under capacity and route length constraints,” *Discrete Optimization*, vol. 12, pp. 129–146, 2014.
- [27] E. Benavent and A. Martínez, “Multi-depot multiple tsp: a polyhedral study and computational results,” *Annals of Operations Research*, vol. 207, pp. 7–25, 2013.
- [28] R. Lahyani, A.-L. Gouguenheim, and L. C. Coelho, “A hybrid adaptive large neighbourhood search for multi-depot open vehicle routing problems,” *International Journal of Production Research*, vol. 57, no. 22, pp. 6963–6976, 2019.
- [29] J.-F. Cordeau, M. Gendreau, and G. Laporte, “A tabu search heuristic for periodic and multi-depot vehicle routing problems,” *Networks: An International Journal*, vol. 30, no. 2, pp. 105–119, 1997.
- [30] J. W. Escobar, R. Linfati, P. Toth, and M. G. Baldoquin, “A hybrid granular tabu search algorithm for the multi-depot vehicle routing problem,” *Journal of Heuristics*, vol. 20, pp. 483–509, 2014.
- [31] F. Scarselli, M. Gori, A. C. Tsoi, M. Hagenbuchner, and G. Monfardini, “The graph neural network model,” *IEEE Transactions on Neural Networks*, vol. 20, no. 1, pp. 61–80, 2008.
- [32] T. N. Kipf and M. Welling, “Semi-supervised classification with graph convolutional networks,” *arXiv preprint arXiv:1609.02907*, 2016.
- [33] A. Vaswani, N. Shazeer, N. Parmar, J. Uszkoreit, L. Jones, A. N. Gomez, E. Kaiser, and I. Polosukhin, “Attention is all you need,” *Advances in Neural Information Processing Systems*, vol. 30, 2017.
- [34] X. Li, W. Luo, M. Yuan, J. Wang, J. Lu, J. Wang, J. Lü, and J. Zeng, “Learning to optimize industry-scale dynamic pickup and delivery problems,” in *2021 IEEE 37th International Conference on Data Engineering (ICDE)*. IEEE, 2021, pp. 2511–2522.
- [35] H. Wen, Y. Lin, X. Mao, F. Wu, Y. Zhao, H. Wang, J. Zheng, L. Wu, H. Hu, and H. Wan, “Graph2route: A dynamic spatial-temporal graph neural network for pick-up and delivery route prediction,” in *Proceedings of the 28th ACM SIGKDD Conference on Knowledge Discovery and Data Mining*, 2022, pp. 4143–4152.
- [36] A. Nowak, D. Folqué, and J. Bruna, “Divide and conquer networks,” in *International Conference on Learning Representations*, 2018.
- [37] S. Li, Z. Yan, and C. Wu, “Learning to delegate for large-scale vehicle routing,” *Advances in Neural Information Processing Systems*, vol. 34, pp. 26 198–26 211, 2021.

- [38] Z. Zong, H. Wang, J. Wang, M. Zheng, and Y. Li, "Rbg: Hierarchically solving large-scale routing problems in logistic systems via reinforcement learning," in *Proceedings of the 28th ACM SIGKDD Conference on Knowledge Discovery and Data Mining*, 2022, pp. 4648–4658.
- [39] Z.-H. Fu, K.-B. Qiu, and H. Zha, "Generalize a small pre-trained model to arbitrarily large tsp instances," in *Proceedings of the AAAI Conference on Artificial Intelligence*, vol. 35, no. 8, 2021, pp. 7474–7482.
- [40] L. Xin, W. Song, Z. Cao, and J. Zhang, "Multi-decoder attention model with embedding glimpse for solving vehicle routing problems," in *Proceedings of the AAAI Conference on Artificial Intelligence*, vol. 35, no. 13, 2021, pp. 12 042–12 049.
- [41] Y.-D. Kwon, J. Choo, B. Kim, I. Yoon, Y. Gwon, and S. Min, "POMO: Policy optimization with multiple optima for reinforcement learning," *Advances in Neural Information Processing Systems*, vol. 33, pp. 21 188–21 198, 2020.
- [42] N. A. Wouda, L. Lan, and W. Kool, "PyVRP: a high-performance VRP solver package," *INFORMS Journal on Computing*, 2024. [Online]. Available: <https://doi.org/10.1287/ijoc.2023.0055>
- [43] N. Christofides and S. Eilon, "An algorithm for the vehicle-dispatching problem," *Journal of the Operational Research Society*, vol. 20, no. 3, pp. 309–318, 1969.
- [44] I.-M. Chao, B. L. Golden, and E. Wasil, "A new heuristic for the multi-depot vehicle routing problem that improves upon best-known solutions," *American Journal of Mathematical and Management Sciences*, vol. 13, no. 3-4, pp. 371–406, 1993.